Intermittent-like Synchronization and Desynchronization Phenomena in a Colpitts Network Model

Victor E. Camargo,[1, a)] Patrick Louodop,[2, 3] Hilda A. Cerdeira,[4] and Fernando F. Ferreira[1]
[1)]*Department of Physics-FFCLRP, University of São Paulo, Ribeirao Preto-SP, 14040-901, Brasil.*
[2)]*Research Unit Condensed Matter, Electronics and Signal Processing, University of Dschang, P.O. Box 67 Dschang, Cameroon.*
[3)]*MoCLiS Research Group, Dschang, Cameroon*
[4)]*São Paulo State University (UNESP), Instituto de Física Teórica, Rua Dr. Bento Teobaldo Ferraz 271, Bloco II, Barra Funda, 01140-070 São Paulo, Brazil.*

(Dated: 4 April 2024)

This study investigates the dynamics of a modified Colpitts oscillator, exhibiting complex periodic and chaotic behaviors. Our research explores the dynamics and synchronization of coupled chaotic Colpitts oscillators, crucial for understanding their potential applications and behaviors. The main discovery is the emergence of a phase in which the systems either achieve complete synchronization or desynchronization. This behavior depends on the values of the coupling parameter. The subsequent challenge involves understanding how the coupling parameter influences the emergence of this synchronization phenomenon.

The study of complex networks and synchronized systems holds immense significance in both technological and natural contexts. Our manuscript explores the intriguing dynamics of a modified Colpitts electrical oscillator, a system known for its simplicity yet capable of exhibiting intricate behaviors. The main results of our research lie in revealing the intermittent synchronization within such a network and the pivotal role of the coupling parameter. Utilizing Master Stability Function (MSF), we obtained a critical bifurcation threshold, offering new insights into the system's behavior under varying conditions. The observed power-law relationship between synchronization and coupling parameters hints at potential universality in complex networks. This research contributes significantly to the field, providing a foundation for future studies and practical applications in designing and controlling synchronized systems.

I. INTRODUCTION

The Colpitts oscillator was invented by Edwin H. Colpitts before 1918 and consists in a combination of inductors (L) and capacitors (C) to produce an oscillation of a certain frequency[1]. Colpitts oscillator is commonly used to generate periodic signals[2] or used as a chaotic oscillator which can generate noise-like broadband signals[3]. The motivation to study Colpitts oscillator is due to the applications in communications[4] and radar systems[5]. Moreover, the underlying properties are characterized by a very rich dynamics[6–9]. The standard Colpitts oscillators incapacity to produce a higher fundamental frequency in a chaotic regime motivated researchers to propose improvements. Some examples are the two-stage Colpitts oscillator[10] and the double-transistor[11]. The fundamental frequency can be tuned from kilohertz to several gigahertz (the microwave range)[12].

Colpitts oscillators display a broad range of complex behavior. Chaotic dynamics in the context of Colpitts oscillators is characterized by only one positive Lyapunov exponent and it was studied in[3,8]. Hyperchaotic dynamical system is characterized for having more than one positive Lyaponov exponent. A hyperchaotic Colpitts circuit was built by[12], they show that hyperchaotic output appears for weak coupled oscillators. Another improved Colpitts oscillator revealed a larger set of interesting phenomena including antimonotonicity, coexistence of attractors and metastable chaos[13].

Here we study the dynamical properties of a Colpitts oscillator without equilibrium points as well as the phase synchronization features of a network of such oscillators. In the standard Colpitts model, the nonlinearity is based on an exponential function or a piecewise linear function[8,13,14] which are unbounded as they can grow indefinitly and can be a source of instability. In this designed Colpitts circuit, the nonlinearity is well bounded and we are still observing qualitatively the same dynamical behavior as periodicity or chaos depending on the selected parameters. The advantage of the present version is the simplicity in the mathematical model that presents only three parameters within which two are related to voltages that are in the electrical circuit, hence they can be perfect for tuning the dynamics of the system. The model is later applied in a network and we investigate the phase synchronization of the ensemble of nodes. Between the desynchronized phase and the fully synchronized phase, we identified another phase in which the system is completely synchronized or desynchronized as a function of the coupling parameter.

The main contribution of this work lies in the identification and characterization of a region of intermittency between synchronized and desynchronized states for a wide range of the coupling parameter (k_1). For low values of k_1, the system is completely desynchronized. However, for high values of $k_1 > k_1^c$, the system can be fully synchronized (where k_1^c is the critical value for synchronization). In the intermittency

[a)]Electronic mail: victor.camargo11@usp.br

region, the system either synchronizes or desynchronizes depending on the value of the coupling parameter. This implies that synchronization in this region depends on $k_1 > k_1^c$, but seemingly in an unpredictable manner. Unlike studied systems where the transition to synchronization occurs from a bifurcation point, here, an intermediate phase arises in which synchronization unexpectedly occurs for a specific $k_1 > k_1^c$ value, and with a small variation in the coupling parameter, the system desynchronizes.

In the subsequent sections, we embark into a comprehensive exploration of our study. Section II provides a presentation of the model, elucidating the dynamic properties of a single oscillator. Following this, in Section III, we examine the collective behavior within a ring topology network, utilizing the modified Colpitts model outlined in the preceding section. The ensuing Section IV encapsulates our discussion, while our conclusive findings are encapsulated in Section V. Additionally, we offer a continuum approximation study of the signum function in the appendix A.

II. COLPITTS OSCILLATOR

Below, in Fig. 1, we present a simplified schematic chart of the Colpitts oscillator[15]. The nonlinearity in this oscillator is based on either an exponential function or a piecewise linear function[8,13,14], both of which are unbounded and can lead to indefinite growth of variables, thus introducing a source of instability.

In this designed Colpitts circuits, the nonlinearity is more precisely defined, and we observe qualitatively the same dynamic behaviors of chaos or periodicity, depending on the chosen parameters. The advantage of the current version lies in the simplicity of the mathematical model, which involves just three parameters. Two of these parameters are related to the voltage present in the electrical circuits, making it easier to adjust the system's dynamics.

The primary contributor to the chaotic behavior in the system is the device shown in Fig. 1(b), known as the operational amplifier (Op-Amp). This circuit is designed to compare the voltage level, V_A and V_B, across the capacitors with a reference voltage V_{ref}. In other words, this operational amplifier is tasked with comparing the magnitudes of two different voltage inputs and determining which one is larger. Its output is bipolar and equals $\pm V$, depending on the relative values of V_{ref}, V_A, and V_B. The outputs of the Op-Amp comparators, V_{S1} from (OA_1) and the output V_{S2} from (OA_2), are then given by

$$\begin{cases} V_{S1} = V_{CC} sgn(V_{ref} - V_B), \\ V_{S2} = V_{CC} sgn(V_{ref} + V_A), \end{cases} \tag{1}$$

where $V_{cc} = V^+ = |V^-|$ is the power supply of the operational amplifiers and *sgn* represent the signum function.

This approach utilizes a voltage comparator based on an operational amplifier to generate the nonlinear term. The expression for nonlinearity, either *sgn* or *tanh*, derives from the Op-Amp's operation. Electrically, the power supply voltage V_{cc},

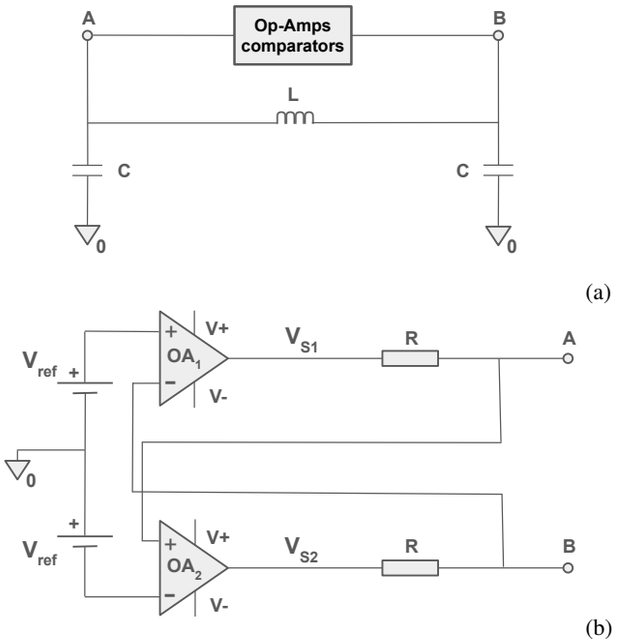

FIG. 1. Circuit diagram. On the upper panel (a) we show the Colpitts circuit, while in the lower panel (b) we show the operational amplifier (Op-Amp) responsible for nonlinearity of the system.

the resistor R, and the reference voltage V_{ref} are independent. Therefore, they can all serve as control parameters. However, only the reference voltage is easily adjustable in practice.

We denote the current flowing through the inductor L as I_L, and the variables V_A and V_B represent the voltages on the capacitors connected to points A and B, respectively. Kirchhoff's laws are applied to the circuit illustrated in Fig. 1 so we can define the dimensionless state variables x, y, and z, where $V_A = x$, $V_B = y$, and $RI_L = z$. Furthermore, the time constant is denoted by $\tau = RC$ and $\beta = \frac{R^2 C}{L}$. Also from now on we write the voltage variables as $V_{cc} = v_{cc}$ and $V_{ref} = v_{ref}$.

The mathematical model depends on the current orientation in the circuit as shown in Fig. 1(a), where the output of OA_1 is directed to the positive entry of OA_2 while the output of OA_2 is going to the negative entry of OA_1. The dimensionless equations of the presented circuit are defined by the following differential equations:

$$\begin{cases} \dot{x} = -x - z + v_{cc} sgn(v_{ref} - y), \\ \dot{y} = -y + z + v_{cc} sgn(v_{ref} + x), \\ \dot{z} = \beta (x - y). \end{cases} \tag{2}$$

Figure 2 illustrates the complex dynamical behavior of the Colpitts oscillator in a three-dimensional phase space, with the axes representing the variables $x(t)$, $y(t)$, and $z(t)$. This graphical representation captures the essence of the chaotic attractors generated by the system. The intricate structure of the attractor suggests that the attractor is chaotic. As we will

see later the corresponded maximum Lyapunov exponent is $\lambda \approx 1.144$. These dynamics are a direct consequence of the nonlinear interactions within the circuit, particularly the role of the Op-Amp comparators in modulating the voltage levels, as dictated by the differential equations in Eq. 2. This plot emphasizes the symmetry inherent in the system's design, while also acknowledging the potential for complex, asymmetric dynamic patterns to emerge due to the orientation of current flow in the circuit. Such a representation is vital for understanding the fundamental nature of the oscillator's chaotic behavior and lays the groundwork for further analysis and application in synchronization and signal processing technologies.

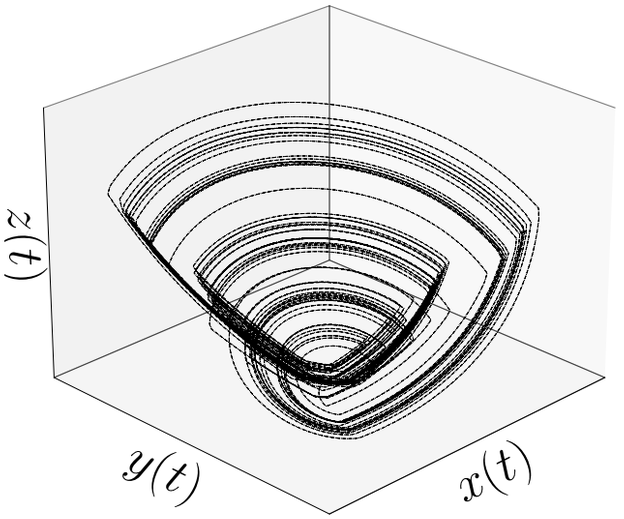

FIG. 2. Temporal evolution of the state variables $x(t)$, $y(t)$, and $z(t)$ associated with the system Eq. (2) for the following fixed values: $v_{cc} = 5$, $v_{ref} = 0.1$, and $\beta = 5$.

To accurately analyze the dynamical properties of the Colpitts oscillator, it is essential to consider the role of Lyapunov exponents. These exponents measure the divergence or convergence rates of trajectories in close proximity within the phase space, serving as a determinant for the system's behavior. Specifically, the system's chaotic or nonchaotic nature is determined by the maximum characteristic Lyapunov exponent. A positive maximum exponent is indicative of chaotic dynamics, signifying sensitive dependence on initial conditions and divergence of nearby trajectories. Conversely, a negative maximum exponent signals stability and convergence towards an attractor. Importantly, the scenario in which the largest Lyapunov exponent is zero, often encountered in practical applications, denotes a critical state of the system where it neither exhibits chaotic behavior nor converges, representing a boundary or transition state between order and chaos.

In the computation of Lyapunov exponents for systems characterized by piecewise smooth dynamics, such as those involving a signum function $sgn(x)$, a significant challenge arises due to the nondifferentiability at points where state variables have zero values ($x = 0$). To address this issue, we introduce a Gaussian approximation of the Dirac delta function, denoted as $\delta_\varepsilon(x)$, which is mathematically expressed as:

$$\delta_\varepsilon(x) = \frac{1}{\varepsilon\sqrt{\pi}} e^{-x^2/\varepsilon^2}, \tag{3}$$

where ε is a small, positive parameter that controls the width of the Gaussian. This formulation allows $\delta_\varepsilon(x)$ to serve as a differentiable stand-in for the Dirac delta function, particularly at $x = 0$, where differentiability is lost. Importantly, the convergence of this approximation to the Dirac delta function is captured by the limit expression:

$$\lim_{\varepsilon \to 0} \delta_\varepsilon(x) = \delta(x), \tag{4}$$

where $\delta(x)$ represents the Dirac delta function. This approach facilitates a refined analysis of the dynamical behavior of the system by leveraging standard differential calculus tools, enabling its use in analytical and numerical methods that require differentiability. All the numerical calculations were performed using a fourth-order Runge-Kutta method (RK4) with a time step of $h = 0.01$, demonstrating a global error of order $O(h^4)$, which reflects the accuracy of this method. In all simulations, the calculations we done with 5×10^4 time iterations, of which 4×10^4 time iterations were allocated to transient solutions.

An analytical dissection of the parameter space reveals the sensitivity of the Colpitts oscillator's dynamics, as seen in Figure 3. By fixing $\beta = 5$ and examining v_{cc} against v_{ref}, the top left bifurcation diagram displays distinct regions of regular and chaotic dynamics. It distinguishes different dynamics from the onset of chaos at points P_a and P_b. Similarly, the v_{cc} versus β diagram, with v_{ref} held constant at 0.1, shows a threshold where slight changes in v_{cc} or β can significantly alter the system's periodicity or trigger chaos, as marked at P_c. Additionally, the interplay between v_{ref} and β, with $v_{cc} = 5$, is depicted in the bottom left plot, highlighting an attractor of chaotic behaviors at point P_d.

The bottom right segment of the Fig. 3 illustrates the distinct dynamics associated with each identified point: P_a, P_b, P_c, and P_d. The phase portraits confirm the oscillator's capacity to exhibit both limit cycles and chaotic attractors. The green areas in the Lyapunov exponents plot signify limit cycle dynamics, indicative of negative exponent values, while the black regions represent chaotic behavior, characterized by positive Lyapunov exponents.

This detailed representation of dynamical states, viewed through the lens of Lyapunov exponents, clearly demonstrates the delicate balance between limit cycles and chaos in the functioning of the oscillator.

III. COLPITTS OSCILLATOR NETWORK

We extend the dynamics of the isolated Colpitts oscillator to a complex network, focusing on the interconnections between

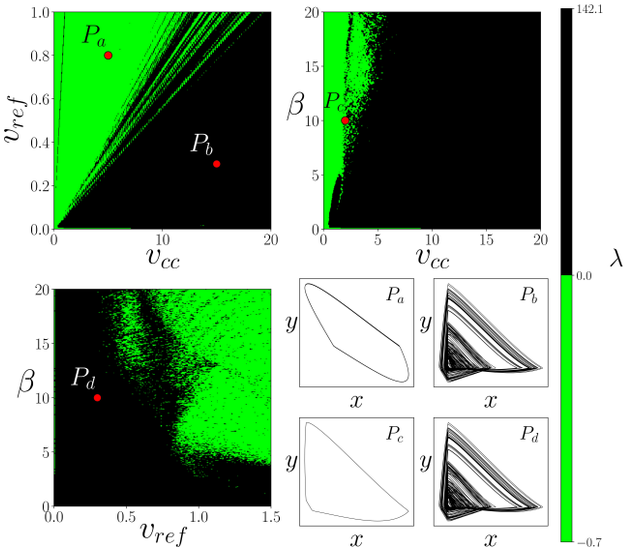

FIG. 3. Comprehensive analysis of the Colpitts oscillator dynamics through maximum Lyapunov exponent (λ) visualization and phase space projections across three parameter spaces: $(v_{cc}, v_{ref}, \beta = 5)$, $(v_{cc}, v_{ref} = 0.1, \beta)$ and $(v_{cc} = 5, v_{ref}, \beta)$. The figure shows the transition from periodic behavior to chaos. The bottom right panels showcase phase space projections at points P_a, P_b, P_c, and P_d, illustrating the oscillator's dynamic range from limit cycles to chaotic attractors.

nodes, which are represented by the voltages at points A and B of the circuit depicted in Fig. 1(a). The coupled differential equations governing this network are as follows:

$$\begin{cases} \dot{x}_i = -x_i - z_i + v_{cc} sgn(v_{ref} - y_i) - k_1(x_i - x_{i-1}), \\ \dot{y}_i = -y_i + z_i + v_{cc} sgn(v_{ref} + x_i) - k_2(y_i - y_{i+1}), \\ \dot{z}_i = \beta(x_i - y_i). \end{cases} \tag{5}$$

In this model, x_i, y_i, and z_i are the state variables of the i-th oscillator in the network of size N. The coupling parameters k_1 and k_2 measure the interaction strength between adjacent oscillators. The network's topology is inspired by real-world electrical networks, characterized by parallel connections, to ensure operational resilience. A notable aspect of this setup is its robustness against failures of individual oscillators; the removal of a single unit does not impair the network's overall functionality, thereby enhancing its fault tolerance.

A. Synchronization

Synchronization in coupled oscillator networks, such as the Colpitts oscillator network, is a critical phenomenon where individual units adjust their states due to interactions, leading to collective dynamics. This subsection focuses on the evolution of synchronization in two coupled oscillators as the coupling strength varies, shedding light on the transition from independent to synchronized behavior and the underlying complexities. Figure 4 showcases the evolution of synchronization between two coupled oscillators within the network as a function of the coupling parameter k_1. The time series for the state variable x is presented for both nodes (x_1 and x_2) across different coupling regimes. At $k_1 = 0$, the oscillators operate independently, with each exhibiting distinct dynamics. As k_1 increases to 0.60, early signs of synchronization emerge, as indicated by the beginning of alignment in the oscillatory patterns of x_1 and x_2, though with noticeable phase and amplitude differences. A further increase to $k_1 = 1.02$ results in near-full synchronization, with the nodes displaying almost identical trajectories. However, at $k_1 = 1.07$, instead of maintaining synchronization, the system exhibits intermittency, oscillating between synchronized and desynchronized states. This phenomenon highlights a complex interaction between synchronization and desynchronization, characteristic of the intermittent transition in the network dynamics.

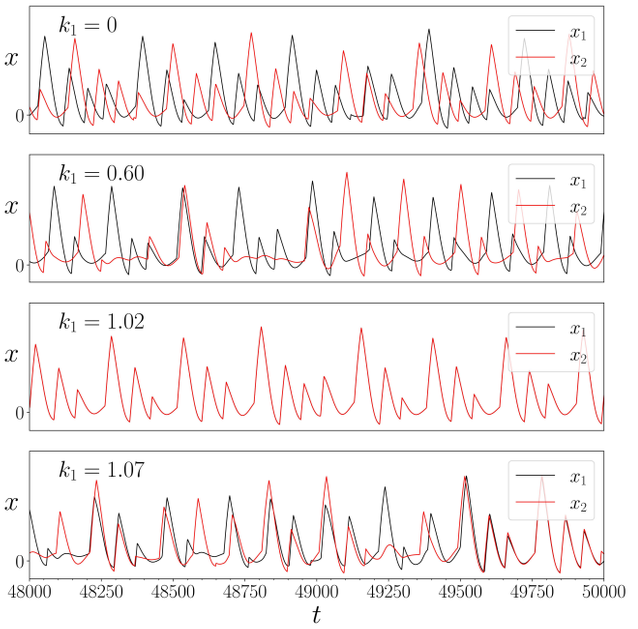

FIG. 4. Time series for a network of $N = 2$ nodes, illustrating the impact of varying the coupling parameter k_1 on the state variable x. The plot captures the transition from desynchronization to near-complete synchronization and back to desynchronization, indicative of intermittency as k_1 changes.

In order to characterize the possible states of synchronization in the system, we consider the asymptotic standard deviation $\langle\sigma\rangle$, calculated after discarding a number of transient states. This is based on the instantaneous standard deviation σ_t across all oscillators $x_i(t), y_i(t), z_i(t)$ for $i = 1 \ldots N$, defined as

$$\sigma_t = \left[\frac{1}{N} \sum_{i=1}^{N} (x_i(t) - \bar{x}(t))^2 + (y_i(t) - \bar{y}(t))^2 + (z_i(t) - \bar{z}(t))^2 \right]^{1/2}, \tag{6}$$

where $\bar{x}$, $\bar{y}$, and $\bar{z}$ are the mean values of the state variables across the network at time t.

The asymptotic standard deviation is then given by

$$\langle \sigma \rangle = \frac{1}{T} \sum_{t=1}^{T} \sigma_t, \tag{7}$$

where T is the total number of time steps considered after the transient time. A synchronized state in the network is indicated by $\langle \sigma \rangle = 0$, denoting that all variables (x_i, y_i, z_i) across the network are in complete synchronization. This condition reflects a state where the trajectories of all oscillators converge to a single trajectory in the phase space, representing a stringent criterion for synchronization.

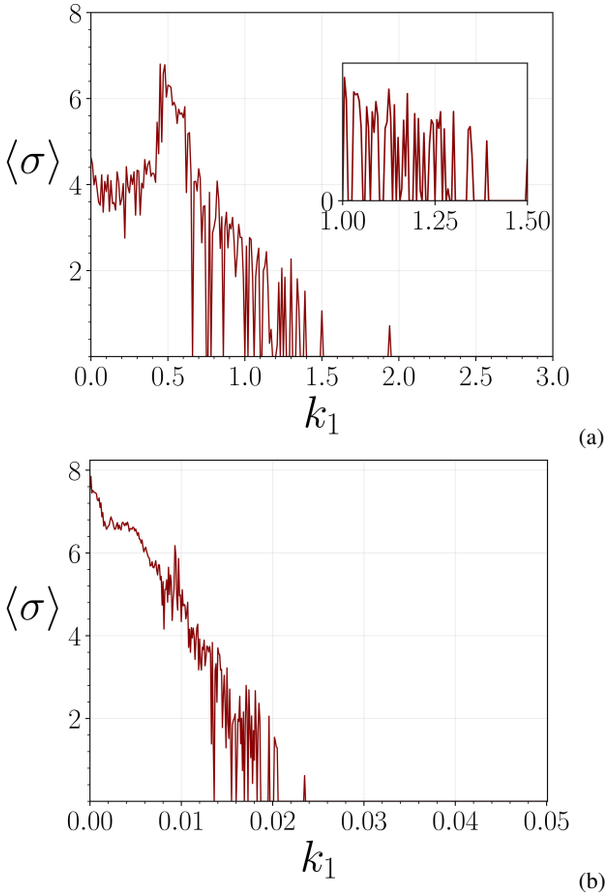

FIG. 5. On the upper panel (a) we show the asymptotic standard deviation $\langle \sigma \rangle$ as a function of the coupling parameter k_1 for $N = 2$ oscillators. A marked decrease in $\langle \sigma \rangle$ is observed as k_1 is increased, indicating a trend towards synchronization in the network. The inset provides a magnified view of the k_1 range from 1.00 to 1.50, highlighting the behavior of $\langle \sigma \rangle$ that suggests the presence of intermittent synchronization. In the lower panel (b) we show the asymptotic standard deviation for $N = 100$ oscillators.

The compelling visualization in Figure 5(a) elucidates the intricate relationship between the coupling parameter k_1 and the network's synchronization, as quantified by the asymptotic standard deviation $\langle \sigma \rangle$. The primary plot reveals a general trend: as k_1 increases, $\langle \sigma \rangle$ notably decreases, indicating a progression towards a synchronized state across the network. Initially, high peaks in $\langle \sigma \rangle$ reflect significant desynchronization, which gradually diminishes with the increase in k_1, suggesting an emergent collective coherence among the oscillators. A particularly striking behavior of $\langle \sigma \rangle$ is observed. Here, sharp and sudden peaks, juxtaposed with swift declines, outline a distinct pattern of intermittency as a function of the coupling parameter. An inset provides a detailed view of the k_1 interval from 1.00 to 1.50, highlighting this phenomenon. This observed intermittency, emerging as a direct consequence of varying k_1, represents a novel pattern; it differs from traditional intermittency over time. The pronounced effect of the signum function likely plays a role in this dynamic, inducing abrupt transitions between synchronized and desynchronized states within the network. In order to verify that this phenomenon occurs for a more complex network, we calculate the asymptotic standard deviation for a network of $N = 100$ as seen in Figure 5(b), in which we observe the same pattern as for $N = 2$ coupled oscillators.

To further explore the impact of the signum function on the network's dynamics, our study is extended in the appendix A. We consider the behavior under the influence of a continuous signum function, specifically the hyperbolic tangent and a custom continuous signum function "S"[16]. These investigations aim to assess the effects of smoothing transitions induced by the signum function. Our goal is to determine whether a less aggressive function can alleviate the observed intermittency, providing a more gradual transition between states and potentially unveiling new dynamics within the network.

We now investigate the standard deviation $\langle \sigma \rangle$ as a function of the coupling parameter k_1 across various step sizes Δk_1, as seen in Figure 6. This analysis is crucial to ascertain whether the observed intermittency is an intrinsic feature of the system's dynamics rather than a byproduct of our sampling resolution. Intriguingly, the system exhibits a power-law behavior in the count of synchronized states Ω as a function of Δk_1. Such a relationship is often associated with scale-invariance and indicative of robust underlying dynamical processes. The emergence of this power-law behavior is significant, as it suggests the presence of universal characteristics in the synchronization patterns. These are typically observed at critical thresholds, where systems undergo phase transitions.

In our comprehensive investigation of the synchronization behavior, particularly of $\langle \sigma \rangle$, we conduct a detailed analysis across four parameter spaces: k_1 versus v_{cc}, k_1 versus v_{ref}, k_1 versus β, and k_1 versus k_2. In Figure 7, the phase diagrams encompass the entire parameter space, shedding light on the intermittent behavior within the system. This extensive mapping is instrumental in understanding the complex interdependencies and the dynamics governing synchronization in the network.

B. Stability of Synchronized States

Understanding the stability of synchronized states is critical in analyzing the dynamics of coupled oscillators. For an

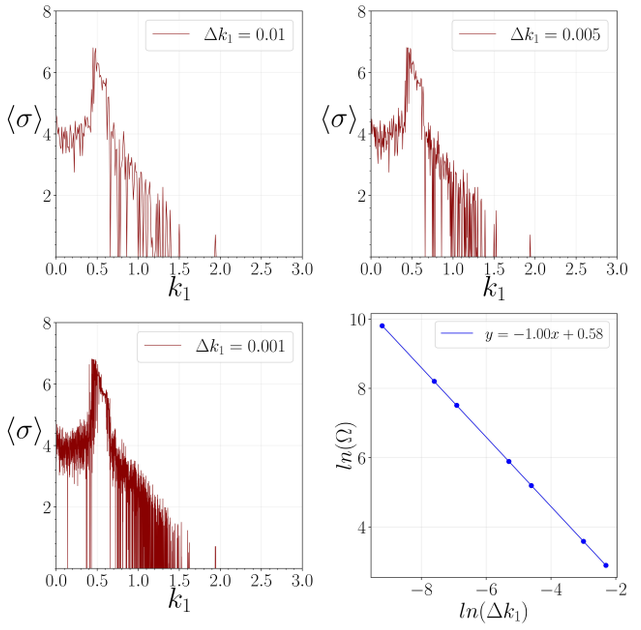

FIG. 6. Synchronization diagram of the system, as described by Eq. (5), for a network of $N = 2$ nodes as a function of various steps of the coupling parameter k_1. The bottom right plot illustrates the count of the synchronized states Ω with respect to Δk_1, revealing a power-law behavior that underscores the scale-invariant nature of the synchronization process.

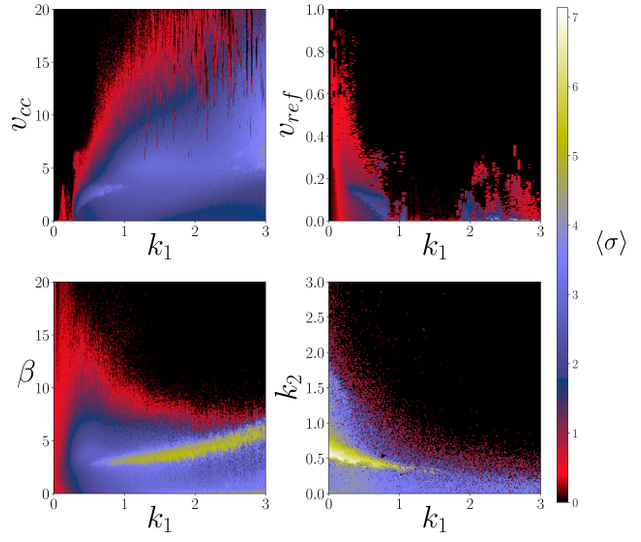

FIG. 7. Synchronization $\langle\sigma\rangle$ across four parameter spaces: (k_1, v_{cc}), (k_1, v_{ref}), (k_1, β), and (k_1, k_2), with fixed values for each scenario: $(v_{ref} = 0.1, \beta = 5)$, $(v_{cc} = 5, \beta = 5)$, $(v_{cc} = 5, v_{ref} = 0.1)$, and $(v_{cc} = 15, v_{ref} = 0.3, \beta = 10.0)$ respectively. These diagrams, derived from the coupled dynamics as described by Eq. (5), showcase the extensive mapping of synchronization states and highlight the prevalence of intermittency within the system.

isolated Colpitts oscillator, its dynamics can be encapsulated in a generalized form as follows:

$$\dot{\mathbf{x}} = \mathbf{F}(\mathbf{x}), \tag{8}$$

where $\mathbf{x}$ is an m-dimensional state vector representing the oscillator's state variables, and $\mathbf{F}(\mathbf{x})$ delineates the oscillator's local dynamics. This framework sets the stage for exploring the conditions under which synchronized states remain stable in a network of coupled oscillators. For constructing a network of N interconnected Colpitts oscillators, we employ the Master Stability Function framework, as introduced by Pecora and Carroll[17]. This approach combines a network topology coupling matrix $\mathbf{G}$, a local dynamics coupling function $\mathbf{H}(\mathbf{x})$, and a scalar coupling parameter ξ. The coupled dynamics for each oscillator in the network are then described by:

$$\dot{\mathbf{x}}_i = \mathbf{F}(\mathbf{x}_i) - \xi \sum_{j=1}^{N} G_{ij}\mathbf{H}(\mathbf{x}_i), \tag{9}$$

where the matrix $\mathbf{G}$ adheres to the zero row-sum condition $\sum_{j=1}^{N} G_{ij} = 0$ for all i, thereby characterizing the coupling structure of the network. This framework is crucial for analyzing the stability and synchronization behavior of the network, taking into account the interplay between the individual oscillators' dynamics and the network topology.

To investigate the stability of the synchronized state $\mathbf{x}_s$ in the network, we introduce perturbations $\delta\mathbf{x}_i(t)$ to each network node:

$$\mathbf{x}_i(t) = \mathbf{x}_s(t) + \delta\mathbf{x}_i(t), \tag{10}$$

a first-order Taylor expansion of Equation (9) is then performed, leading to the Jacobian matrices $\mathbf{DF}(\mathbf{x}_s)$ and $\mathbf{DH}(\mathbf{x}_s)$. The perturbations $\delta\mathbf{x}_i(t)$ evolve according to the variational equations evaluated at the synchronized state $\mathbf{x}_s(t)$:

$$\delta\dot{\mathbf{x}}_i = \mathbf{DF}(\mathbf{x}_s)\delta\mathbf{x}_i - \xi \sum_{j=1}^{N} G_{ij}\mathbf{DH}(\mathbf{x}_s)\delta\mathbf{x}_j, \tag{11}$$

In accordance with Pecora and Carroll's methodology[17], this equation (11) can be decoupled into N independent eigenmodes, resulting in a block-diagonal form:

$$\dot{\mathbf{v}}_i = [\mathbf{DF}(\mathbf{x}_s) - \xi\mu_i\mathbf{DH}(\mathbf{x}_s)]\,\mathbf{v}_i, \tag{12}$$

where μ_i represent the eigenvalues of the matrix $\mathbf{G}$, with $i = 1, 2, \ldots, N$, and $\mathbf{v}_i$ denotes the distinct perturbation modes of the synchronized state. Analyzing the stability of these modes is essential for determining the robustness of synchronization across the oscillator network.

The Master Stability Function (MSF), denoted as λ_T, provides critical insights into the stability of synchronized states within a network of coupled Colpitts oscillators. As depicted in Figure 8, the MSF illustrates a critical transition at $k_1 = 1$. The change in sign from negative to positive values at this point signifies a shift from stable to unstable synchronization. Notably, this transition point coincides with the intermittent

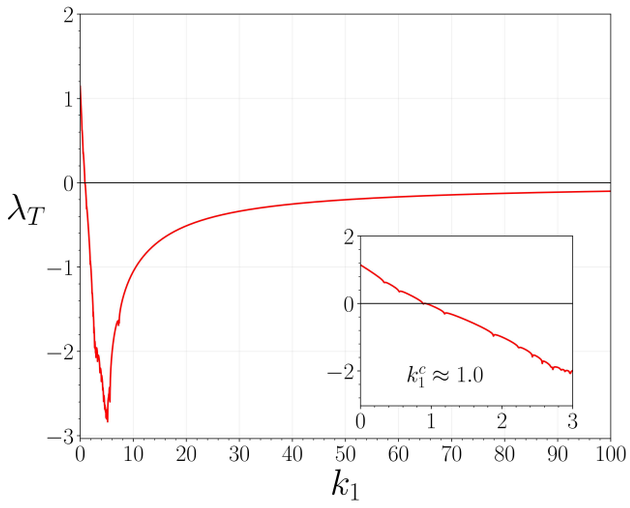

FIG. 8. The Master Stability Function (MSF) λ_T depicted as a function of the coupling parameter k_1 for a network of $N = 2$ Colpitts oscillators. The inset highlights the critical point where λ_T changes sign at $k_1 = 1$, correlating with the observed intermittency in standard deviation.

behavior observed in the network, suggesting a direct link between the coupling parameter and the onset of synchronization.

In the region where λ_T is negative (for $k_1 < 1$), the network experiences robust synchronization, with perturbations gradually diminishing over time, thereby reinforcing the synchronized state. On the other hand, when λ_T becomes positive (for $k_1 > 1$), perturbations tend to amplify, leading to desynchronization within the network. The inset in the figure highlights this pivotal juncture at $k_1 = 1$, delineating the boundary between these two distinct dynamical behaviors.

The behavior of the MSF is particularly telling, as it emphasizes the network's sensitivity to changes in the coupling parameter. This sensitivity is characteristic of systems with complex dynamics, such as coupled Colpitts oscillators, where the state of synchronization is crucial to the overall system behavior. Analyzing the MSF in relation to k_1 not only deepens our understanding of synchronization phenomena but also acts as a valuable predictive tool for assessing the stability of synchronized states under varying coupling strengths.

The graphical representations in Figure 9 provide a comprehensive overview of the stability of synchronized states across a range of system parameters. The color-coded Master Stability Function (MSF) values act as clear indicators of stability: black regions indicate stable synchronization for $\lambda_T < -0.03$; red regions represent areas where the network may be desynchronized, yet the MSF is negative and close to zero for $-0.03 < \lambda_T < 0$; green regions signify potential synchronization with MSF positive and close to zero for $0 < \lambda_T < 0.03$; and yellow regions denote instability for $\lambda_T > 0.03$ therefore full desynchronization. Finally, the regions with green and red colors correspond to situations in which the MSF may fail to predict the synchronization, that is, regions of MSF inaccuracy, as discussed in Huang et al. (2009)[18]. This visual

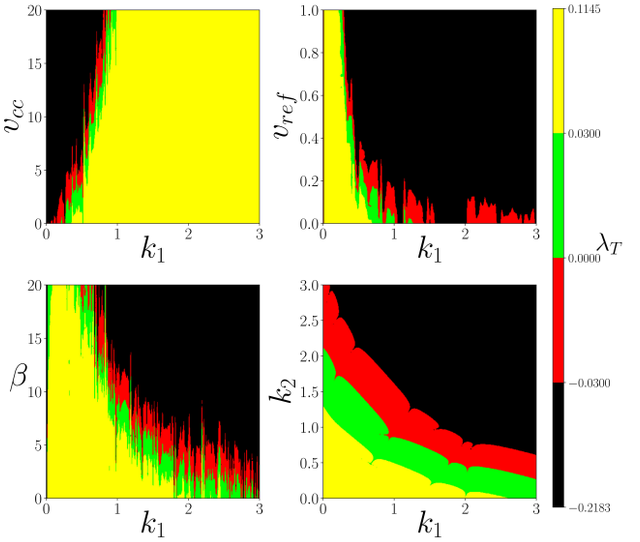

FIG. 9. Master Stability Function (λ_T) mapped over four parameter spaces: (k_1, v_{cc}), (k_1, v_{ref}), (k_1, β), and (k_1, k_2), with fixed parameter sets: $(v_{ref} = 0.1, \beta = 5)$, $(v_{cc} = 5, \beta = 5)$, $(v_{cc} = 5, v_{ref} = 0.1)$, and $(v_{cc} = 15, v_{ref} = 0.3, \beta = 10.0)$ respectively, applied to the coupled Colpitts oscillator dynamics as per Eq. (5). Yellow regions denote instability for $\lambda_T > 0.03$, leading to full desynchronization; green regions signify potential synchronization with MSF positive and close to zero for $0 < \lambda_T < 0.03$; red regions represent areas where the network may be desynchronized, yet the MSF is negative and close to zero for $-0.03 < \lambda_T < 0$; black regions indicate stable synchronization for $\lambda_T < -0.03$.

analysis aligns with the insights gained from earlier synchronization phase diagrams, emphasizing the critical role of the coupling parameter k_1 and its interaction with other system parameters in influencing the emergence and persistence of synchronized behavior within the network.

A particularly noteworthy aspect of these phase diagrams is the transition regions where λ_T changes from negative to positive, especially around $k_1 = 1$. This shift mirrors the intermittent synchronization behavior observed in the standard deviation plots, highlighting the intricate complexity of the system's dynamics. By comparatively studying these diagrams, we gain a deeper understanding of the specific conditions under which the Colpitts oscillator network attains or loses synchrony. This knowledge provides a valuable roadmap for potential control and optimization strategies in these dynamic systems.

IV. DISCUSSION

The comprehensive analysis conducted herein has revealed significant insights into the synchronization dynamics of a conceived Colpitts oscillator network. The core of this investigation revolved around the intricate phenomenon of intermittency in synchronization, a characteristic underscored by the fluctuations in the synchronization measure $\langle\sigma\rangle$ and manifested as abrupt transitions within the network's phase space.

Following this, we observed in Figure 5 (a) that the system is desynchronized when the coupling strength $k_1 < 0.5$ and it is completely synchronized for $k_1 > 2$. In the interval $0.5 < k_1 < 2$, we found a phase with alternation between synchronization and desynchronization in a very irregular manner. The observed pattern of synchronization or desynchronization in the system occurs irregularly or randomly, depending on the coupling parameter values. This bears resemblance to the pattern or phenomenon known as intermittency. Therefore, we will refer to it as intermittent-like. The alternating patterns of synchronization and desynchronization states are induced by certain factors or conditions within a system, which emerge as a result of nonlinear interactions.

A detailed examination of multiple Lyapunov phase spaces for each system parameter has shed light on the stability landscape of the network, revealing a complex dynamical system where synchronization is exquisitely sensitive to the nuances of the coupling parameter k_1. This sensitivity was quantitatively captured through the discovery of a power-law relationship, highlighting that minor variations in k_1 can lead to substantial effects on the network's synchrony. This confirms that intermittency is not merely a consequence of our sampling resolution but a fundamental feature of the system's dynamics.

The use of the Master Stability Function (MSF) has been pivotal in quantifying the stability of synchronized states. Through its lens, we identified regions within the parameter space where the network exhibited stable synchronization, alongside regimes prone to desynchronization. The transition between these domains is crucial for understanding the behavior of the Colpitts oscillator network and leveraging its dynamics for practical applications. Particularly intriguing is the observation of a critical change in the sign of the MSF at $k_1 = 1$, indicative of a transition from stable to unstable synchronization. This juncture aligns with the principles outlined by Pecora and Carroll, highlighting systems' propensity for unstable behaviors near such critical points.

The vicinity of $k_1 = 1$ emerges as a bifurcation threshold where the system's response to perturbations becomes highly sensitive, potentially leading to the intermittent synchronization patterns observed. This transition zone, marked by the MSF's sign change, heralds the complex dynamics where the system unpredictably oscillates between coherence and incoherence phases. Such critical points are of paramount interest, offering insights into the nuanced interplay between the network's structure and its emergent behavior.

Additionally, our analysis revealed some discrepancies between Figure 7 and Figure 9, echoing findings by Huang et al. (2009)[18], which observed desynchronization with negative MSF eigenvalues near zero. This underscores the MSF method's limited predictive power for synchronization under certain conditions. Huang et al. suggested that the accuracy of MSF predictions diminishes with eigenvalues near zero, pointing to the necessity for a broader analytical framework beyond the maximum Lyapunov exponent. This insight underscores the need for refining the MSF method to more accurately capture the synchronization dynamics of complex networks.

V. CONCLUSION

In conclusion, this investigation into the Colpitts oscillator model has yielded profound insights into its synchronization dynamics. The study has moved the discourse beyond classical synchronization scenarios, unveiling the presence of intermittent synchronization as a direct consequence of the coupling parameter's variability. The nuanced understanding of this intermittency, especially in relation to the MSF's delineation of stability, is a testament to the depth of analysis achieved.

The power-law behavior associated with the changes in the steps of the coupling parameter k_1 marks an important advancement in our comprehension of how such systems can be tuned and controlled. It indicates a potential universality in the behavior of complex networks, a concept that can be leveraged for the design and control of various technological and natural systems.

As we look to the future, the insights gleaned from this research will undoubtedly inform the development of more resilient and adaptable networks. The intricate balance between stability and flexibility observed in the Colpitts oscillator network exemplifies the delicate interplay that any engineered or natural synchronized system must navigate. It is this balance that will inspire ongoing and future research, pushing the boundaries of our understanding of complex, synchronized systems.

VI. DATA AVAILABILITY STATEMENT

The data that supports the findings of this study are available within this article.

VII. ACKNOWLEDGMENT

Victor Camargo is grateful to CAPES for doctoral fellowship: "This study was financed in part by the Coordenação de Aperfeiçoamento de Pessoal de Nível Superior – Brasil (CAPES) – Finance Code 001." PL and HAC thank ICTP-SAIFR and FAPESP grant 2021/14335-0 for partial support

Appendix A: Comparative Analysis of Sigmoid Functions in Network Synchronization

In the main sections of this study, we noted a pronounced intermittency in the synchronization measure $\langle\sigma\rangle$ as a function of the coupling parameter k_1. This intermittency is characterized by sharp peaks and rapid declines, a behavior that is particularly unusual as it arises directly from the variation of k_1, contrasting with typical temporal intermittency observed in dynamical systems.

The pronounced discontinuity of the signum function is hypothesized to significantly contribute to the observed dynamic, by inducing abrupt transitions in state. To explore the impact of function smoothness on synchronization, we extend

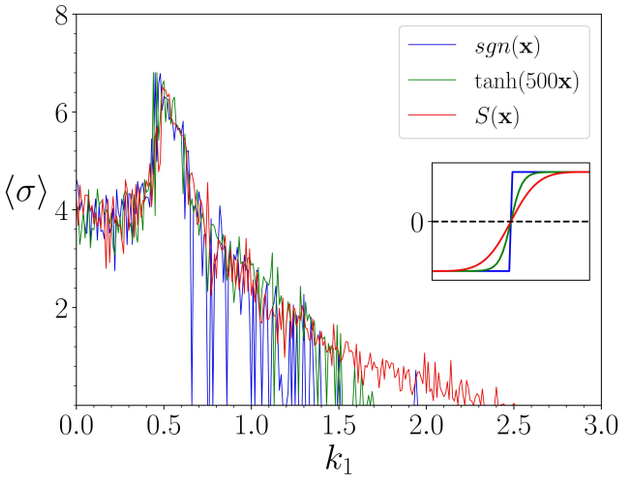

FIG. 10. Comparison of the average synchronization standard deviation $\langle\sigma\rangle$ for different coupling functions within the Colpitts oscillator network for $N = 2$. The functions compared are the standard signum function $sgn(x)$, the hyperbolic tangent $\tanh(nx)$ with $n = 500$, and a continuous approximation of the signum function $S(x)$ with parameter $b = 120$. The inset showcases the functional forms and their impact on synchronization.

our analysis to include the hyperbolic tangent function and a specially formulated continuous signum function $S(x)$[16], defined as:

$$S(x) = \frac{(1+x)^b - (1-x)^b}{(1+x)^b + (1-x)^b}, \tag{A1}$$

where x is the input signal and b modulates the smoothness of the transition. Higher values of b result in a steeper function.

Our findings, depicted in Figure 10, reveal that $S(x)$ offers a notably smoother transition between synchronization states compared to $sgn(x)$. The parameter b is adjusted to 120 to exemplify a less abrupt yet decisive change in state. The hyperbolic tangent, set with $n = 500$, also demonstrates a smoother profile, but it does not achieve the subtlety of transition exhibited by $S(x)$. This comparative analysis suggests that the continuous nature of $S(x)$ might alleviate the sharpness of intermittency, leading to more gradual transitions. This characteristic could be particularly advantageous in applications where smooth synchronization dynamics are essential.

The hyperbolic tangent function is notable for its smooth yet rapid transition characteristics. The phase diagram shown in Figure 11 captures the synchronization behavior within a network of Colpitts oscillators, where the hyperbolic tangent function is used as the coupling mechanism. The parameter n quantifies the sharpness of the hyperbolic tangent function, influencing the rate at which it transitions from -1 to 1 as its input crosses from negative to positive values. The horizontal axis, k_1, represents the coupling strength among the oscillators. The color coding in the diagram indicates the magnitude of the synchronization error $\langle\sigma\rangle$.

Interestingly, the diagram reveals regions where certain combinations of parameters facilitate complete synchronization. Conversely, areas with high variability in $\langle\sigma\rangle$ indicate regimes where the network tends to desynchronize and exhibit intermittency. These transitions between regimes are particularly pronounced with variations in k_1, highlighting the significant influence of coupling strength on the network's collective dynamics.

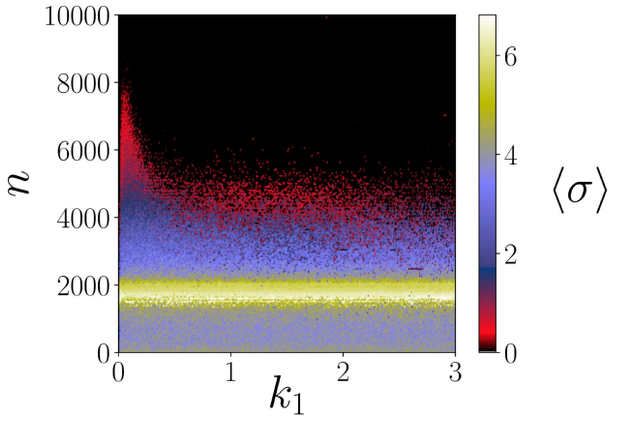

FIG. 11. Phase space of synchronization characterized by the average synchronization standard deviation $\langle\sigma\rangle$ as a function of the coupling parameter k_1 and the sharpness parameter n of the hyperbolic tangent function for a network of $N = 2$ coupled oscillators.

Considering now the continuous signum function $S(x)$, which provides a smooth transition between states, the phase diagram depicted in Figure 12 illustrates the synchronization standard deviation $\langle\sigma\rangle$ across various values of the coupling parameter k_1 and the smoothness parameter b of $S(x)$.

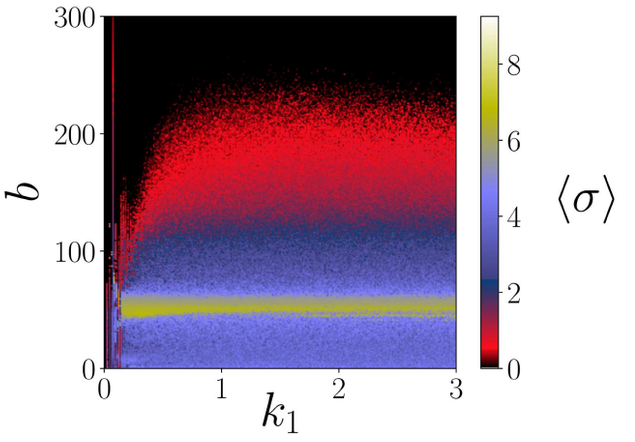

FIG. 12. Synchronization phase space showing the average standard deviation $\langle\sigma\rangle$ in relation to the coupling parameter k_1 and the smoothness parameter b of the continuous signum function $S(x)$ for a network of $N = 2$ coupled oscillators.

The parameter b determines the steepness of $S(x)$, effectively controlling the function's degree of nonlinearity. The continuous nature of $S(x)$ results in smoother gradients of synchronization across the phase space, indicating that the tran-

sitions induced by $S(x)$ are less abrupt compared to those of the standard signum function. This characteristic potentially allows for enhanced control over the network's synchronized behavior. The value of b is critical in fine-tuning these transitions; lower values lead to broader transitions, while higher values result in sharper changes.

The analysis of this phase diagram provides valuable insights into the impact of the continuous function $S(x)$ on synchronization. It suggests that by adjusting b, the network can achieve a more refined control over its synchronized state, potentially offering significant implications for the design and stabilization of complex oscillator networks.

REFERENCES

[1]C. H, "Oscillation generator," (1927), uS Patent 1,624,537.
[2]M. P. Kennedy, "Chaos in the colpitts oscillator," IEEE Transactions on Circuits and Systems I: Fundamental Theory and Applications **41**, 771–774 (1994).
[3]G. M. Maggio, O. De Feo, and M. P. Kennedy, "Nonlinear analysis of the colpitts oscillator and applications to design," IEEE Transactions on Circuits and Systems I: Fundamental Theory and Applications **46**, 1118–1130 (1999).
[4]A. Uchida, M. Kawano, and S. Yoshimori, "Dual synchronization of chaos in colpitts electronic oscillators and its applications for communications," Physical review E **68**, 056207 (2003).
[5]S. Qiao, Z.-G. Shi, T. Jiang, and L.-X. Ran, "A new architecture of uwb radar utilizing microwave chaotic signals and chaos synchronization," Progress In Electromagnetics Research **75**, 225–237 (2007).
[6]G. Mykolaitis, A. Tamasevicius, A. Cenys, S. Bumelien, A. N. Anagnostopoulos, and N. Kalkan, "Very high and ultrahigh frequency hyperchaotic oscillators with delay line," Chaos, Solitons & Fractals **17**, 343–347 (2003).
[7]L. Guo-Hui, "Synchronization and anti-synchronization of colpitts oscillators using active control," Chaos, Solitons & Fractals **26**, 87–93 (2005).
[8]J. Effa, B. Essimbi, and J. M. Ngundam, "Synchronization of improved chaotic colpitts oscillators using nonlinear feedback control," Nonlinear Dynamics **58**, 39 (2009).
[9]R. Bonetti, S. De Souza, A. Batista, J. Szezech Jr, I. Caldas, R. Viana, S. Lopes, and M. Baptista, "Super persistent transient in a master–slave configuration with colpitts oscillators," Journal of Physics A: Mathematical and Theoretical **47**, 405101 (2014).
[10]A. Tamaševičius, G. Mykolaitis, S. Bumelienė, A. Čenys, A. Anagnostopoulos, and E. Lindberg, "Two-stage chaotic colpitts oscillator," Electronics Letters **37**, 549–551 (2001).
[11]A. Tamasevicius, S. Bumeliene, and E. Lindberg, "Improved chaotic colpitts oscillator for ultrahigh frequencies," Electronics Letters **40**, 1569–1570 (2004).
[12]A. Čenys, A. Tamasevicius, A. Baziliauskas, R. Krivickas, and E. Lindberg, "Hyperchaos in coupled colpitts oscillators," Chaos, Solitons & Fractals **17**, 349–353 (2003).
[13]V. Kamdoum Tamba, H. Fotsin, J. Kengne, E. B. Megam Ngouonkadi, and P. Talla, "Emergence of complex dynamical behaviors in improved colpitts oscillators: antimonotonicity, coexisting attractors, and metastable chaos," International Journal of Dynamics and Control **5**, 395–406 (2017).
[14]J. Kengne, J. Chedjou, G. Kenne, and K. Kyamakya, "Dynamical properties and chaos synchronization of improved colpitts oscillators," Communications in Nonlinear Science and Numerical Simulation **17**, 2914–2923 (2012).
[15]M. Kountchou, V. F. Signing, R. T. Mogue, J. Kengne, P. Louodop, *et al.*, "Complex dynamic behaviors in a new colpitts oscillator topology based on a voltage comparator," AEU-International Journal of Electronics and Communications **116**, 153072 (2020).
[16]J. Zhang, Y. Zhang, W. Ali, *et al.*, "Linearization modeling for non-smooth dynamical systems with approximated scalar sign function," in *2011 50th IEEE Conference on Decision and Control and European Control Conference* (IEEE, 2011) pp. 5205–5210.
[17]L. M. Pecora and T. L. Carroll, "Master stability functions for synchronized coupled systems," Physical review letters **80**, 2109 (1998).
[18]L. Huang, Q. Chen, Y.-C. Lai, and L. M. Pecora, "Generic behavior of master-stability functions in coupled nonlinear dynamical systems," Physical Review E **80**, 036204 (2009).